Nanoscale architecture dictates detection profile of surface-confined DNA by MALDI-TOF MS

ARTICLE *in* ANALYTICAL CHEMISTRY · SEPTEMBER 2009

Impact Factor: 5.64 · DOI: 10.1021/ac901815v · Source: PubMed

5 AUTHORS, INCLUDING:

Min Hong
Liaocheng Universtiy
55 PUBLICATIONS **325** CITATIONS
SEE PROFILE

Xin Zhou
Southeast University (China)
11 PUBLICATIONS **166** CITATIONS
SEE PROFILE

Anal. Chem. **2009,** *81,* 8839–8845

Nanoscale Architecture Dictates Detection Profile of Surface-Confined DNA by MALDI-TOF MS

Min Hong,[†,‡] Xin Zhou,[†] Jiping Li,[†] Yuan Tian,[†] and Jin Zhu*[,†]

Department of Polymer Science and Engineering, State Key Laboratory of Coordination Chemistry, Nanjing National Laboratory of Microstructures, School of Chemistry and Chemical Engineering, Nanjing University, Nanjing 210093, China, and Department of Chemistry, Liaocheng University, Liaocheng 252059, China

The design and fabrication of various nanoscale architectures for the effective MALDI-TOF MS analysis of surface-confined DNA are reported. The nanoscale architectures are derived from layer-by-layer assemblies of negatively charged nanoparticles and positively charged polymers. An important finding is that porous structures comprising bottom SiO_2 nanoparticle layers and top Au nanoparticle layers enable the observation of both covalently bound (with Au−S bond) and hybridized oligonucleotides. The achievement of this unprecedented detection capability is attributed to the unique combination of a nanoporous dielectric film and discrete noble metal nanoparticles. The conclusion is supported by control experiments performed on a variety of single and multilayered Au nanoparticle structures, where only the hybridized oligonucleotides in a two- or three-strand system could be detected.

In the fields of molecular biology and biochemistry, as well as in the practical diagnosis of diseases, DNA hybridization has become a powerful tool for the isolation, detection, and analysis of specific oligonucleotide sequences.[1] Typically, such hybridization assays utilize oligonucleotide probes that have been immobilized on a solid support.[2,3] The detection of biomolecular interactions (DNA hybridization or DNA-derived interactions in particular) is important for unraveling the complex phenomena inside cells. Monolayer technology (e.g., DNA microarrays[4]) provides the platform for probing and digesting such kinds of interactions. To accurately investigate the hybridization process (e.g., hybridization efficiency) and other DNA-mediated biomolecular interactions, the analysis of immobilized probes is of utmost importance.[5] On-chip synthesis and chemical reactivity of DNA can be probed through a highly efficient method for the analysis of immobilized strands.[6] In fact, in many cases, mass spectrometry (MS) has been used as the primary analytical tool for the structural determination of DNA-based reactions in solution.[7] Overall, the ability to analyze all the DNA components in a surface-confined format is important for improving the performance and utility of DNA arrays for practical applications (e.g., biosensing). Herein, we demonstrated, for the first time, the ability to detect immobilized DNA with matrix-assisted laser desorption/ionization time-of-flight mass spectrometry (MALDI-TOF MS) through the fabrication of appropriate nanoscale architectures. A surface-confined three-strand DNA hybridization system has been fully probed, with all the strands detected simultaneously. Therefore, our work represents an important step toward the understanding of surface-confined DNA structures. Potential applications of the method described herein include, but are not limited to, the assay of chemical reactivity, structure integrity, and biomolecular interactions associated with DNA.

Several approaches for the analysis of DNA hybridization with immobilized probes have been developed. For example, surface plasmon resonance (SPR) spectroscopy[8a−c] and quartz crystal microbalance (QCM)[8d] have provided a hint of the reactivity associated with double-strand DNA (ds-DNA) and single-strand DNA (ss-DNA). Imaging X-ray photoelectron spectroscopy (XPS) and imaging time-of flight secondary ion mass spectrometry (TOF-SIMS) are complementary, sensitive tools for the analysis of elemental composition, chemical structure, relative density, and

* To whom correspondence should be addressed. Phone: +86 25-8368-6291. Fax: +86 25-8331-7761. E-mail: jinz@nju.edu.cn.

[†] Nanjing University.

[‡] Liaocheng University.

(1) (a) Alivisatos, P. *Nat. Biotechnol.* **2004**, *22*, 47–52. (b) Ho, H.-A.; Najari, A.; Leclerc, M. *Acc. Chem. Res.* **2008**, *41*, 168–178.

(2) (a) Saiki, R. K.; Walsh, P. S.; Levenson, C. H.; Erlich, H. A *Proc. Natl. Acad. Sci. U.S.A.* **1989**, *86*, 6230–6234. (b) Drmanac, R.; Labat, I.; Brukner, I.; Crkvenjakov, R. *Genomics* **1989**, *4*, 114–128. (c) Strezoska, Z.; Paunesku, T.; Radosavljevic, D.; Labat, I.; Drmanac, R.; Crkvenjakov, R. *Proc. Natl. Acad. Sci. U.S.A.* **1991**, *88*, 10089–10093. (d) Pease, A. C.; Solas, D.; Sullivan, E. J.; Cronin, M. T.; Holmes, C. P.; Fodor, S. P. A. *Proc. Natl. Acad. Sci. U.S.A.* **1994**, *91*, 5022–5026.

(3) (a) ODonnell, M. J.; Tang, K.; Koster, H.; Smith, C. L.; Cantor, C. R. *Anal. Chem.* **1997**, *69*, 2438–2443. (b) Tsubery, H.; Mrksich, M. *Langmuir* **2008**, *24*, 5433–5438.

(4) (a) Fodor, S. P. A.; Read, J. L.; Pirrung, M. C.; Stryer, L.; Lu, A. T.; Solas, D. *Science* **1991**, *251*, 767–773. (b) Pirrung, M. C. *Angew. Chem., Int. Ed.* **2002**, *41*, 1276–1289.

(5) Chrisey, L. A.; Lee, G. U.; O'Ferrall, C. E. *Nucleic Acids Res.* **1996**, *24*, 3031–3039.

(6) (a) Ban, L.; Mrksich, M. *Angew. Chem., Int. Ed.* **2008**, *47*, 3396–3399. (b) Marin, V. L.; Bayburt, T. H.; Sligar, S. G.; Mrksich, M. *Angew. Chem., Int. Ed.* **2007**, *46*, 8796–8798. (c) Yeo, W.-S.; Min, D.-H.; Hsieh, R. W.; Greene, G. L.; Mrksich, M. *Angew. Chem., Int. Ed.* **2005**, *44*, 5480–5483. (d) Min, D.-H.; Su, J.; Mrksich, M. *Angew. Chem., Int. Ed.* **2004**, *43*, 5973–5977. (e) Su, J.; Mrksich, M. *Angew. Chem., Int. Ed.* **2002**, *41*, 4715–4718.

(7) See, for example:(a) Tse, B. N.; Snyder, T. M.; Shen, Y.; Liu, D. R. *J. Am. Chem. Soc.* **2008**, *130*, 15611–15626. (b) Rozeman, M. M.; Kanan, M. W.; Liu, D. R. *J. Am. Chem. Soc.* **2007**, *129*, 14933–14938. (c) Snyder, T. M.; Liu, D. R. *Angew. Chem., Int. Ed.* **2005**, *44*, 7379–7382.

(8) (a) Buckle, M.; Williams, R. M.; Negroni, M.; Buc, H *Proc. Natl. Acad. Sci. U.S.A.* **1996**, *93*, 889–894. (b) Brockman, J. M.; Nelson, B. P.; Corn, R. M. *Annu. Rev. Phys. Chem.* **2000**, *51*, 41–63. (c) Niikura, K.; Matsuno, H.; Okahata, Y. *J. Am. Chem. Soc.* **1998**, *120*, 8537–8538. (d) Wang, J.; Jiang, M.; Palecek, E. *Bioelectrochem. Bioenerg.* **1999**, *48*, 477–480.

10.1021/ac901815v CCC: $40.75
Published on Web 09/28/2009

spatial distribution of DNA arrays on solid substrates.[9] However, none of these tools provide the requisite accurate information regarding the complete molecular structure of the immobilized species. The small quantity that is typically accessible for DNA renders it impossible to characterize the structure with nuclear magnetic resonance (NMR). MS has therefore been arguably the method of choice for structural assignments under these circumstances. We have developed an assay format that combines the unique surface chemistry of nanostructures and MALDI-TOF MS, which enables the analysis of DNA immobilization and hybridization events on an exquisitely fabricated, nanoparticle (NP)-assembled substrate.

MALDI-TOF MS has been a diagnostic tool developed primarily for the analysis of biopolymers, such as proteins and nucleic acids.[10,11] To avoid the low ionization efficiency and facile fragmentation of oligonucleotides, earlier reports on the MALDI-TOF MS of DNA are mainly focused on the selection of appropriate matrixes and improvement of sample deposition methods.[12,13] Recently, increasing efforts have been made to selectively extract and preconcentrate DNA samples prior to MS analysis (e.g., with the use of the biotin−streptavidin system).[3b,14] Another approach for purifying DNA samples, which relies on the strong interaction of a chemically modified oligonucleotide on a solid surface, is widely used, such as the anchoring of thiolated DNA on a Au surface through Au−S bond.[15] Although many of these methods were quite successful for their respective applications, direct analysis of DNA strands immobilized covalently on a solid support by MALDI-TOF MS has yet to be reported. Therefore, it is of paramount importance to develop more effective and direct methods for the analysis of such structures. Because Au NP-based solid supports provide large surface area, good biocompatibility, and various surface functionalization possibilities, they have been effectively used for the immobilization of biomolecules and have proven to be excellent substrates in many fields ranging from biosensors to molecular diagnostics.[16,17]

In this paper, we report the design and construction of various NP-based porous nanostructures for effective desorption and analysis of surface-confined DNA by MALDI-TOF MS. To generate nanoporous substrates, alternate layer-by-layer electrostatic adsorption was used to fabricate various Au NP-assembled as well as Au and SiO_2 NP-assembled multilayers on an underlying silicon wafer. These substrates are easy to fabricate and process and can be used for the immobilization of thiolated oligonucleotides on Au NPs. The morphology of the porous structures was carefully examined with scanning electron microscopy (SEM). The immobilization of ss-DNA and two- and three-strand hybridized ds-DNA on the Au NP-based interfaces were studied with MALDI-TOF MS. Remarkably, direct analysis of a covalently bound self-assembled monolayer (SAM) from thiolated oligonucleotides can be routinely carried out on a substrate comprising Au and SiO_2 NPs, besides the identification of hybridized strands. The interaction mechanism between ss-DNA or ds-DNA immobilized, NP-assembled nanoporous substrates and MALDI-TOF MS will be discussed. To verify the validity of our system, a series of Au NP-assembled as well as Au and SiO_2 NP-assembled supports are prepared.

EXPERIMENTAL SECTION

Materials. All materials and reagents were used as received unless otherwise noted. All oligonucleotides (Table S-1) were synthesized and purified by Sangon, Inc. (Shanghai, China), and their concentrations were quantified by optical density (OD) at 260 nm. Capture strand DNA-1 is a thiolated oligonucleotide with an -$(A)_{10}$-spacer at the 3′ end, which complements End strand DNA-2 and part of the Linker sequence of DNA-3. End DNA-4 is complementary to the other part of Linker DNA-3 (for detailed sequences and their respective molecular weight, see Table S-1).

Surface Characterization. SEM characterization was performed on Hitachi S-4800 at 10 kV. MALDI MS spectra of DNAs were obtained using an autoflex II MALDI TOF-TOF mass spectrometer (Bruker-Daltonics, Bremen, Germany) equipped with a Scout-384 source.

Fabrication of $(PDDAC/Au\ NP)_{1-3}/(PDDAC/SiO_2\ NP)_9/(PDDAC/PSS)_5$/PEI Nanostructures on a Si Wafer. Au NPs with an average diameter of 13 nm were synthesized by the citrate reduction of $HAuCl_4$.[18] The silicon wafers were cleaned by treatment with a "Piranha solution" (sulfuric acid/hydrogen peroxide, 70/30 v/v %) at 90 °C for 2 h, and subsequently negatively charged by heating at 70 °C for 20 min in a 5:1:1 (volume ratio) mixture of water, hydrogen peroxide, and 30% ammonia solution. Aqueous solutions of 0.05 wt % SiO_2 NPs, 40 mM (repeat unit basis) poly(ethylene imine) (PEI), 40 mM poly(styrene sulfonate) (PSS), and 40 mM poly(diallyldimethylamonium chloride) (PDDAC) were prepared with deionized (DI) water. Prior to the deposition of first layer SiO_2 NPs, a $(PDDAC/PSS)_5$/PEI prelayer for adhesion purposes was deposited onto each freshly treated Si wafer in order to prepare a dense SiO_2 NP layer. The clean Si wafer was immersed in PEI solution for 5 min and rinsed with DI water in three separate bottles, each for 1 min. The substrate was then softly dried using an argon stream. The PEI-modified Si wafer was alternately dipped in PSS solution and PDDAC solution for 5

(9) Lee, C. Y.; Harbers, G. M.; Grainger, D. W.; Gamble, L. J.; Castner, D. G. *J. Am. Chem. Soc.* **2007**, *129*, 9429–9438.
(10) Karas, M.; Hillenkamp, F. *Anal. Chem.* **1988**, *60*, 2299–2301.
(11) Dass, C. *Principles and Practices of Biological Mass Spectrometry*; Wiley: New York, 2001.
(12) (a) Wu, K. J.; Shaler, T. A.; Becker, C. H. *Anal. Chem.* **1994**, *66*, 1637–1645. (b) Wang, B. H.; Biemann, K. *Anal. Chem.* **1994**, *66*, 1918–1924. (c) Kirpekar, F.; Nordhoff, E.; Kristiansen, K.; Roepstorff, P.; Hahner, S.; Hillenkamp, F. *Rapid Commun. Mass Spectrom.* **1995**, *9*, 525–531.
(13) (a) Liu, Y. H.; Bai, J.; Liang, X.; Lubman, D. M.; Venta, P. *J. Anal. Chem.* **1995**, *67*, 3482–3490. (b) Gut, I. G.; Jeffery, W. A.; Pappin, D. J. C.; Beck, S. *Rapid Commun. Mass Spectrom.* **1997**, *11*, 43–50. (c) Tang, W.; Zhu, L.; Smith, L. M. *Anal. Chem.* **1997**, *69*, 302–312.
(14) (a) Jurinke, C.; van den Boom, D.; Collazo, V.; Luchow, A.; Jacob, A.; Koster, H. *Anal. Chem.* **1997**, *69*, 904–910. (b) Kim, S.; Ruparel, H. D.; Gilliam, T. C.; Ju, J. *Nat. Rev. Genet.* **2003**, *4*, 1001–1008.
(15) (a) Plutowski, U.; Richert, C. *Angew. Chem., Int. Ed.* **2005**, *44*, 621–625. (b) Moses, S.; Brewer, S. H.; Lowe, L. B.; Lappi, S. E.; Gilvey, L. B. G.; Sauthier, M.; Tenent, R. C.; Feldheim, D. L.; Franzen, S. *Langmuir* **2004**, *20*, 11134–11140. (c) Dombi, K. L.; Griesang, N.; Richert, C. *Synthesis* **2002**, 816–824. (d) Petrovykh, D. Y.; Kimura-Suda, H.; Whitman, L. J.; Tarlov, M. J. *J. Am. Chem. Soc.* **2003**, *125*, 5219–5226.
(16) (a) Olofsson, L.; Rindzevicius, T.; Pfeiffer, I.; Kall, M.; Hook, F. *Langmuir* **2003**, *19*, 10414–10419. (b) Lee, S.; Perez-Luna, V. H. *Anal. Chem.* **2005**, *77*, 7204–7211.
(17) (a) Mahmoud, K. A.; Hrapovic, S.; Luong, J. H. T. *ACS Nano* **2008**, *2*, 1051–1057. (b) Mani, V.; Chikkaveeraiah, B. V.; Patel, V.; Gutkind, J. S.; Rusling, J. F. *ACS Nano* **2009**, *3*, 585–594.
(18) Grabar, K. C.; Freeman, R. G.; Hommer, M. B.; Natan, M. *J. Anal. Chem.* **1995**, *67*, 735–743.

min and then rinsed and dried with the method mentioned above. The Si wafer was then dried with an argon stream, and these procedures were repeated five times. The $(PDDAC/PSS)_5$/PEI-coated Si wafer was then immersed in a SiO_2 NP solution and PDDAC solution for 5 min alternately, followed by a final dipping of the substrates into the NP suspension. The porosity of the films can be satisfactorily achieved by increasing the number of PDDAC and SiO_2 NP deposition cycles to nine. Subsequently, the $(PDDAC/SiO_2\ NP)_9/(PDDAC/PSS)_5$/PEI-coated Si wafer was then immersed in a Au NP solution and PDDAC solution for 10 min alternately, followed by a final dipping of the substrates into the Au NP suspension, and washed three times with DI water. Finally, the Au and SiO_2 NPs hybrid porous nanostructures can be obtained with the Au NPs as the outermost layer.

Fabrication of Au NP/Polyelectrolyte Porous Nanostructures on a Si Wafer. The Au NP-assembled multilayers were fabricated with the same "layer-by-layer" method as mentioned above, except for only the use of 40 mM PDDAC aqueous solution and 13 nm Au NP aqueous solution. The porosity of the nanostructures can be satisfactorily achieved by increasing the number of PDDAC and Au NPs deposition cycles (1−12 layers) (Detailed experimental procedure can be found in Supporting Information).

Preparation of Au Film on a Si Wafer. Au films on the single-crystal Si(100) wafer were also used as substrates. Prior to the deposition of the films, the wafers were cleaned using a Piranha solution. After cleaning, a Cr adhesion layer (10 nm) was predeposited by vapor deposition, followed by 100 nm of Au. Each substrate was rinsed thoroughly with DI water and dried with argon stream prior to immobilization of the DNA.

Preparation of DNA Monolayers. SAMs of 3′ thiol-modified Capture DNA-1 on Au NP-based substrates were prepared as described previously. Briefly, various Au NP-coated wafers were immersed in an aqueous solution of Capture DNA-1 at a concentration of 3.04 μM. The monolayers were allowed to form at room temperature for 24 h, rinsed with DI water, and dried under a stream of argon. For hybridization, a solution of complementary oligonucleotide strand in PBS (0.3 M NaCl, 0.01 M sodium phosphate, pH 7.0) was applied to the monolayer presenting the immobilized oligonucleotide for 12 h at ambient temperature, including the End DNA-2 (7.24 μM) and Linker DNA-3 (3.07 μM), which may be followed by a further complementary End DNA-4 (5.1 μM). The monolayer was then washed with PBS to remove nonspecifically bound species and dried under a stream of argon.

RESULTS AND DISCUSSION

A variety of surfaces have been examined as supports for the formation of surface-confined DNA structures, including silicon wafer[19] and metal surfaces (e.g., Au substrate[3b,15]). The direct analysis of oligonucleotides captured by complementary strands covalently bound to silicon surfaces has been reported.[19] In principle, these methods provide sufficient resolution that allows the differentiation of DNA strands of different lengths. However, these substrates rely on either the use of complicated surface organic chemistry, solution organic synthesis, or technically demanding high-temperature annealing. More importantly, in practice, effective analysis of covalently bound oligonuleotide SAM by MALDI-TOF MS has not been realized. MALDI-TOF MS analysis of small organic molecules, carbohydrates, and peptides can be routinely achieved and has been the source of rich information for chemical reactions and molecular interactions.[6]

Two-dimensional (2D) and three-dimensional (3D) self-assembled polyelectrolyte multilayer films have been used for the fabrication of microarrays, which are less than 10 nm thick or above the micrometers level, respectively.[20,21] However, none of them possess the features of both high reproducibility and a lower background signal. A multilayered, polyelectrolyte coating with a thickness of ∼100 nm on a slide substrate for DNA microarrays was prepared, which simultaneously combines the advantages of the 2D monolayer and the 3D thick film coatings and eliminates their disadvantages.[22] In our earlier work, we have described the utilization of a ∼70 nm two-tiered nanostructure, comprising an underlying porous film of a polyelectrolyte/SiO_2 NPs and a top layer of Au NPs, for the successful matrix-free characterization of an organic molecule SAM with LDI-TOF MS.[23] To achieve direct analysis of the oligonucleotide SAM by MALDI-TOF MS, here we report a series of simple procedures to coat silicon wafers with Au NP-containing porous thin films by the self-assembly of ployelectrolyte multilayer films,[22] and the protocols for fabricating DNA hybridization structures with thiolated oligonucleotides as DNA binding probes (Scheme 1).

First, a Au and SiO_2 NP hybrid porous nanostructure was prepared with a monolayer of Au NPs as the outermost structure via layer-by-layer assembly. The $(PDDAC/SiO_2\ NP)_9/(PDDAC/PSS)_5$/PEI-coated silicon wafers were fabricated as the underlying porous substrates. Previous atomic force microscopy (AFM) analysis revealed the thickness of for a $(PDDAC/SiO_2\ NP)_9/(PDDAC/PSS)_5$/PEI film.[23] The root-mean-square surface roughness of the film is approximately 10−15 nm. Correspondingly, the hybrid nanostructure with a monolayer of Au NPs is approximately 80 nm thick. SEM characterization shows that the Au NPs are uniformly dispersed on the SiO_2 NP-assembled structure, while the porosity and the roughness are preserved after the Au NP-capping step (Figure 1A). To demonstrate the utility of the hybrid film for MALDI-TOF MS characterization of DNA SAM and hybridization structures, we selected a thiolated Capture DNA-1 as binding probe (Scheme 1A). In order to improve the accessibility of complementary DNA, long spacer arms of $-(A)_{10}-$ are designed at the 3′ end of the oligonucleotide probes. For MS experiments, there are four types of samples being characterized on these Au NP-monolayer capped hybrid films: (1) Capture DNA-1; (2) Capture DNA-1 + End DNA-2; (3) Capture DNA-1 + Linker DNA-3; (4) Capture DNA-1 + Linker DNA-3 + End DNA-4, where any

(19) (a) Tang, K.; Fu, D.-J.; Julien, D.; Braun, A.; Cantor, C. R.; K-ster, H. *Proc. Natl. Acad. Sci. U.S.A.* **1999**, *96*, 10016–10020. (b) Jin, L.; Horgan, A.; Levicky, R. *Langmuir* **2003**, *19*, 6968–6975.

(20) (a) Rogers, Y. H.; Baucom, P. J.; Huang, Z. J.; Bogdanov, V.; Anderson, S.; Boyce-Jacino, M. T. *Anal. Biochem.* **1999**, *266*, 23–30. (b) Lemeshko, S. V.; Powdrill, T.; Belosludtsev, Y. Y.; Hogan, M. *Nucleic Acids Res.* **2001**, *29*, 3051–3058. (c) Zhao, X. D.; Nampalli, S.; Serino, A. J.; Kumar, S. *Nucleic Acids Res.* **2001**, *29*, 955–959.

(21) (a) Proudnikov, D.; Timofeev, E.; Mirzabekov, A. D. *Anal. Biochem.* **1998**, *159*, 34–41. (b) Kodadek, T. *Chem. Biol.* **2001**, *8*, 105–115.

(22) Zhou, X.; Wu, L.; Zhou, J. *Langmuir* **2004**, *20*, 8877–8885.

(23) Hong, M.; Qiu, F.; Huang, L. L.; Zhu, J. *J. Phys. Chem. C* **2008**, *112*, 11078–11081.

Scheme 1. Schematic Illustration of Analysis of DNA Hybridization Immobilized on the Au and SiO_2 NP-Assembled Hybrid Porous Nanostructure (A), and the Au NP-Assembled Multilayer Film (B) by MALDI-TOF MS

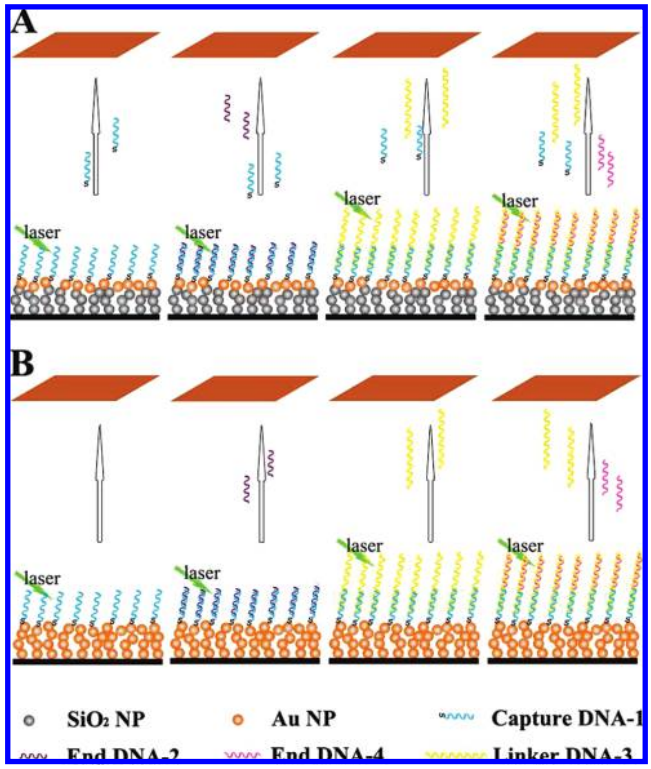

two conjoint oligonucleotides are complementary with each other. In this case, 0.7 M 3-hydroxypicolinic acid (3-HPA) with 70 mM ammonium citrate in 50% acetonitrile was used as the matrix. Ammonium citrate was used for cation exchange to remove excess Na^+ and K^+ ions on the DNA backbone.

Analysis of the monolayer presenting the single-stranded thiolated DNA-1 (Capture DNA-1) revealed a peak at m/z 7927.4, which could be assigned as $[DNA\text{-}1 + 5Na - 4H]^+$ (Figure 2A). This result is in sharp contrast to previous reports,[3b,15] which have failed to observe the oligonucleotides covalently immobilized on Au surfaces by MALDI-TOF MS. We reasoned that is due to the use of Au NPs and the presence of dielectric nanoporous structure. An identical monolayer was then treated with a solution containing the complementary 12-mer strand (End DNA-2), rinsed with PBS buffer, loaded with matrix, and analyzed by MS. The spectrum showed two clear peaks (Figure 2B), with a stronger one (3668.8) corresponding to $[DNA\text{-}2 + Na]^+$, and the weaker one (7983.5) assigned as $[DNA\text{-}1 + 8Na - 7H]^+$. A control experiment using a noncomplementary oligonucleotide (End DNA-4) gave no hybridization signal and ruled out nonspecific interaction of the second oligonucleotide with the monolayer. Additionally, under the same condition, another "Capture DNA-1 + Linker DNA3" hybridization monolayer was also tested, where part of the longer Linker DNA-3 is complementary to Capture DNA-1. As shown in Figure 2C, two peaks are also observed, with the stronger one as $[DNA\text{-}3 + K]^+$ (8435.7), and the weaker one as $[DNA\text{-}1 + 5Na - 4H]^+$ (7927.6). Meanwhile, we characterized the fourth type DNA hybridization monolayer, "Capture DNA-1 + Linker DNA3 + End DNA-4". The third strand 'End DNA-4' is complementary with the other part of Linker DNA-3. As

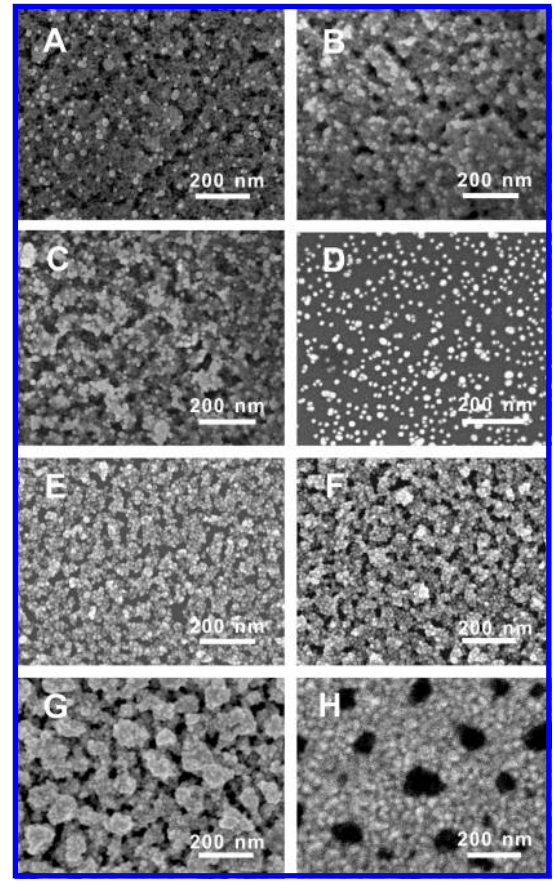

Figure 1. SEM images of the $(PDDAC/Au\ NP)_n/(PDDAC/SiO_2\ NP)_9/(PDDAC/PSS)_5/PEI$ hybrid porous nanostructures, $n = 1$ (A), 2 (B), 3 (C), and the $(PDDAC/Au\ NP)_n$-assembled film, $n = 1$ (D), 3 (E), 9 (F), 12 (G), as well as the ~100 nm thick evaporated Au substrate (H).

expected, three distinct peaks are observed in Figure 2D. Except for two peaks for $[DNA\text{-}3 + K]^+$ (8438.5) and for $[DNA\text{-}1 + 5Na - 4H]^+$ (7921.1), a stronger peak is observed at 3605.8, which can be assigned as $[DNA\text{-}4 + Na]^+$. Signal assignments with different number of counterions observed in this work have also been presented previously.[24] It has been observed that the relative peak intensities of different components can vary from one laser shot to another as well as from one location of the probe surface to another, presumably due to the fluctuation in laser output as well as the inhomogeneity of the matrix crystals distributed on the surface.[25] Thus, it was necessary to hunt for a good spot to get a strong mass signal. In order to obtain an acceptable signal-to-noise ratio on a reflecting TOF system, a higher laser irradiance is usually needed. For all hybridization arrays, a trend of decreasing mass intensity and resolution with the increase of oligonucleotide size was found. A significantly broader profile was observed for the bigger oligomers, Capture DNA-1 and Linker DNA-3, which is in agreement with a previous report.[12a]

To optimize the Au NP dispersion on the underlying SiO_2 NP-assembled porous nanostructure for the construction of DNA arrays, we spotted the Capture DNA-1 probe onto Si wafers

(24) Liu, Y. H.; Bai, J.; Liang, X. L.; Lubman, D. M. *Anal. Chem.* **1995**, *67*, 3482–3490.
(25) Tang, K.; Fu, D. J.; Kotter, S.; Cotter, R. J.; Cantor, C. R.; Koster, H. *Nucleic Acids Res.* **1995**, *23*, 3126–3131.

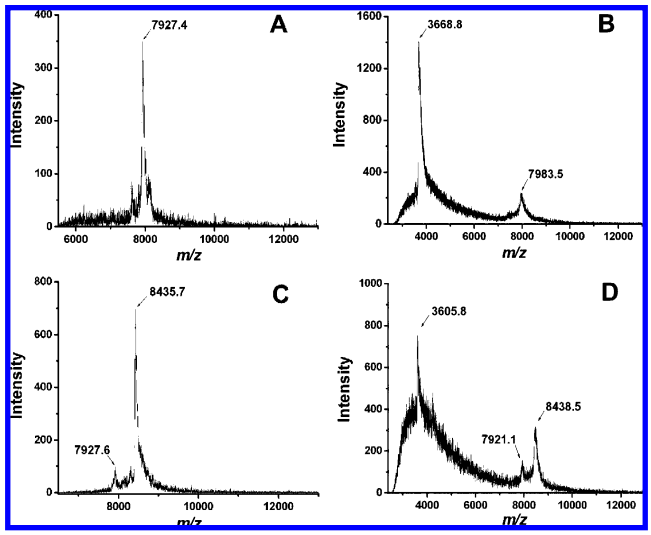

Figure 2. MALDI-TOF MS spectra of the (PDDAC/Au NP)$_1$/(PDDAC/SiO_2 NP)$_9$/ (PDDAC/PSS)$_5$/PEI nanostructures following immobilization of the first thiolated Capture DNA-1 at 7927.4, assigned as [DNA-1 + 5Na − 4H]$^+$ (A), hybridization of the complementary sequence End DNA-2 at 7983.5 and 3668.8, assigned as [DNA-1 + 8Na − 7H]$^+$ and [DNA-2 + Na]$^+$, respectively (B), or hybridization of the complementary longer sequence Linker DNA-3 at 8435.7 and 7927.6, assigned as [DNA-3 + K]$^+$ and [DNA-1 + 5Na − 4H]$^+$, respectively (C), as well as the hybridization of the further complementary strand End DNA-4 at 8438.5, 7921.1 and 3605.8, assigned as [DNA-3 + K]$^+$, [DNA-1 + 5Na − 4H]$^+$, and [DNA-4 + Na]$^+$, respectively (D).

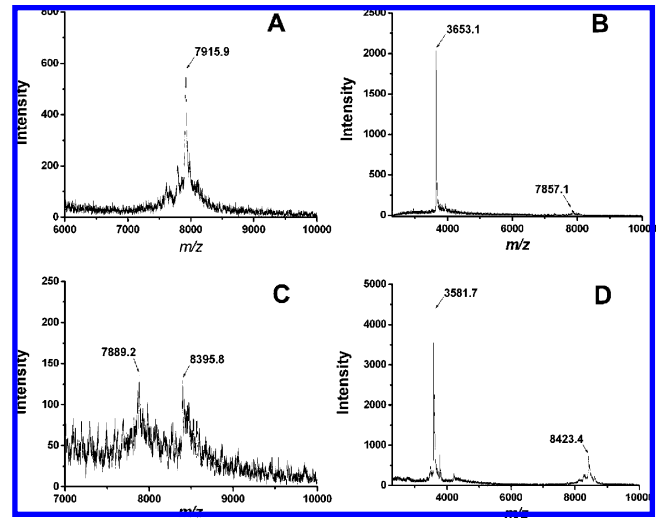

Figure 3. MALDI-TOF MS spectra of the (PDDAC/Au NP)$_3$/(PDDAC/SiO_2 NP)$_9$/ (PDDAC/PSS)$_5$/PEI nanostructures following immobilization of the first thiolated Capture DNA-1 at 7915.9, assigned as [DNA-1 + 5Na − 4H]$^+$ (A), hybridization of the complementary sequence End DNA-2 at 7857.1 and 3653.1, assigned as [DNA-1 + 2Na − H]$^+$ and [DNA-2 + H]$^+$, respectively (B), or hybridization of the complementary longer sequence Linker DNA-3 at 8395.8 and 7889.2, assigned as [DNA-3 + H]$^+$ and [DNA-1 + 4Na − 3H]$^+$, respectively (C), as well as the hybridization of the further complementary strand End DNA-4 at 8423.4 and 3581.7, assigned as [DNA-3 + Na]$^+$ and [DNA-4 + H]$^+$, respectively (D).

that were coated with three bilayers of Au NP/PDDAC. The effects of number *n* of bilayers of Au NP/PDDAC are shown in Figure 1A−C. The Au NP density increased with an increase of the number of bilayer, and aggregation appeared when the bilayer number (*n*) was ~3 (Figure 1C). In this case, four types of DNA samples immobilized on the Au NP three-layer capped hybrid films were studied with MALDI-TOF MS, which include: (1) Capture DNA-1; (2) Capture DNA-1 + End DNA-2; (3) Capture DNA-1 + Linker DNA-3; (4) Capture DNA-1 + Linker DNA-3 + End DNA-4. Similar results (Figure 3) were obtained as observed for the DNA array on the Au NP monolayer-assembled nanostructures, except for the three-strand hybridization systems. The Capture DNA-1 was not observed at all (Figure 3D). Therefore, we conclude that Au NP aggregation is unfavorable for the analysis of the three-strand DNA hybridization array. Because of the existence of the SiO_2 NP-assembled nanoporous structure and individually Au NPs, the signal of covalently immobilized thiolated oligonuleotide in the DNA monolayer or hybridization array can be detected.

From the above experiments, we can see that the existence of SiO_2 NP-assembled nanoporous film and separate Au NPs is critical to the success of the analysis of covalently bound thiolated oligonuleotides by MALDI-TOF MS. To verify the hypothesis, other nanoscale substrates have been investigated. A Au NP-monolayer film on the silicon wafer was prepared first. The SEM micrograph (Figure 1D) shows that uniformly distributed Au NPs on the Si wafer produce an ideal interface under our experimental conditions for further DNA immobilization. Four DNA array systems fabricated as mentioned above have also been analyzed on these Au NP-monolayer-coated wafers. The difference is obvious, as for all three DNA hybridization samples, only the second or third strand could be observed (Figure 4), and we were unable to obtain peaks corresponding to the covalently bound probes in any of the DNA microarrays. Moreover, for three-strand hybridization, the upper two strands can be observed simultaneously.

The thickness of the coating film deposited on the support is also an important factor for microarray performance. Au NP/polyelectrolyte-assembled porous nanostructures were studied for their characteristics related to the MALDI-TOF MS of the single-strand oligonucleotide SAM and DNA hybridization array (Scheme 1B). Parts E, F, and G of Figure 1 show the contrast of the Au NP assembly morphology on Si wafers that were coated with three, nine, and twelve bilayers of Au NP/PDDAC. The Au NP aggregation increased with the increase of the number of bilayer, and aggregation obviously appeared when the bilayer number (*n*) exceeded ~3 (Figure 1E). The surfaces of nine and twelve bilayers of Au NP/PDDAC were selected for analysis of the DNA hybridization array because they commonly present porous structures similar to the morphology of Au and SiO_2 NP-assembled hybrid nanoporous films (Figures 1F,G).

In addition, one significant observation was that Au NPs have packed closely into the bulk and few separate NPs were found for the Au NP-assembled twelve-layer films. Figures 5 and S-1 show the MS of three types of DNA hybridization systems on the nine and twelve bilayers of Au NP/PDDAC, respectively, which are similar to those observed on the Au NP-monolayer-coated wafers. Although the porosity results in a larger binding capacity of the thiolated oligonucleotide on the surfaces of Au NP-assembled multilayer films as compared to Au NP-monolayer, there was no signal detected for the covalently bound DNA on any of the Au NP-assembled nanoporous films. Besides, from the comparison of MS signals provided by the Au NP-assembled mono-, nine-, and twelve-layer films, we can see that the "shapes"

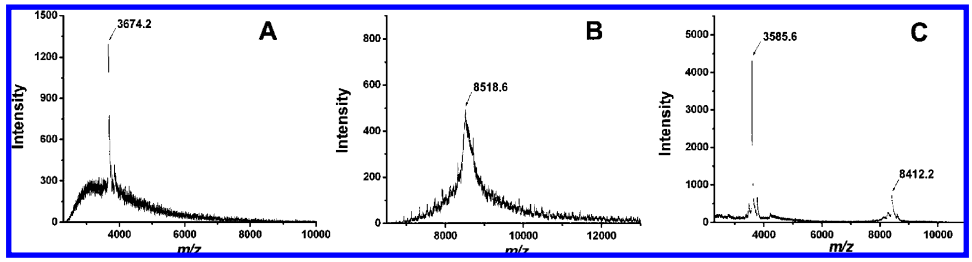

Figure 4. MALDI-TOF MS spectra of three types of DNA hybridization arrays on the Au NP-assembled monolayer on Si wafer: (1) Capture DNA-1 + End DNA-2, at 3674.2, assigned as $[DNA\text{-}2 + Na]^+$ (A); (2) Capture DNA-1 + Linker DNA-3, at 8518.6, assigned as $[DNA\text{-}3 + 2K + 2Na - 3H]^+$ (B); (3) Capture DNA-1 + Linker DNA-3 + End DNA-4, at 8412.2 and 3585.6, assigned as $[DNA\text{-}3 + Na]^+$ and $[DNA\text{-}4 + H]^+$, respectively (C).

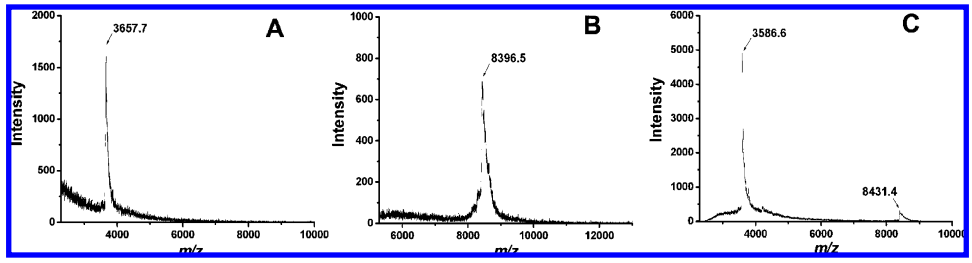

Figure 5. MALDI-TOF MS spectra of three types of DNA hybridization arrays on the Au NP-assembled nine-layer on Si wafer: (1) Capture DNA-1 + End DNA-2, at 3657.7, assigned as $[DNA\text{-}2 + H]^+$ (A); (2) Capture DNA-1 + Linker DNA-3, at 8396.5, assigned as $[DNA\text{-}3 + H]^+$ (B); (3) Capture DNA-1 + Linker DNA-3 + End DNA-4, at 8431.4 and 3586.6, assigned as $[DNA\text{-}3 + K]^+$ and $[DNA\text{-}4 + H]^+$, respectively (C).

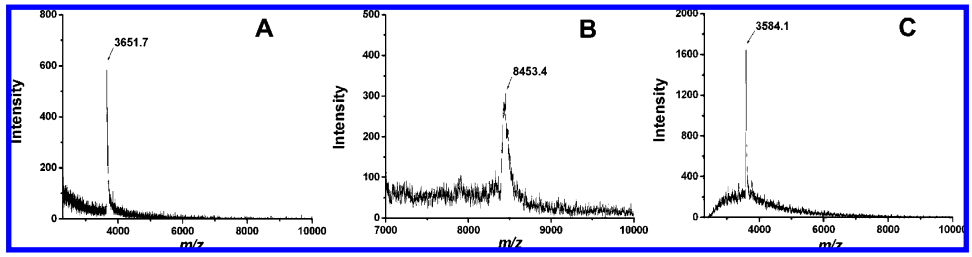

Figure 6. MALDI-TOF MS spectra of three types of DNA hybridization arrays on the Au substrates: (1) Capture DNA-1 + End DNA-2, at 3651.7, assigned as $[DNA\text{-}2 + H]^+$ (A); (2) Capture DNA-1 + Linker DNA-3, at 8453.4, assigned as $[DNA\text{-}3 + 3Na - 2H]^+$ (B); (3) Capture DNA-1 + Linker DNA-3 + End DNA-4, at 3584.1, assigned as $[DNA\text{-}4 + H]^+$ (C).

and "sizes" of NP-based porous structures have little effect, under the experimental conditions employed herein, on the DNA MALDI-TOF MS data.

Similar results were also obtained for the analysis of DNA hybridization samples on the Au substrates, which were prepared by thermal evaporation of the Cr adhesion layer (10 nm), followed by Au (100 nm), onto the silicon wafers. The SEM characterization shows that closely packed Au particles occupy the entire surface of support, and there are a few pores interspersing the Au surface (Figure 1H). These pores are obviously larger than those presented in the Au NP-assembled multilayer films or Au and SiO_2 NP-assembled hybrid films. Therefore, the density of surface-bound oligonucleotide probes and their accessibility to a complementary strand during the hybridization process on the Au substrates are markedly lower than those of the layer-by-layer-assembled nanoporous films. This led to not only an absence of the peak corresponding to the covalently immobilized oligonucleotides but also the weaker intensity of the second (Figures 6A,B) or third hybridization strand (Figure 6C).

Taken together, all the data indicate that individual Au NPs and the underlying SiO_2 NP-assembled porous nanostructure are the two key factors for the full analysis of the DNA hybridization array by MALDI-TOF MS, including the signal of covalently bound probes. This is consistent with the result reported from our previous work.[23] When Au NP aggregation occurs, the energy that Au NPs adsorb from the laser irradiation will be transferred and diffused to the neighboring Au, and this prevents efficient energy transfer to the analytes immobilized on the surface. Accordingly, as Au NPs were captured on the insulating SiO_2 NP-assembled nanoporous film, effective energy transfer was realized, and this is favorable for the desorption of covalently bound oligonucleotides.

CONCLUSIONS

In summary, we have demonstrated the use of layer-by-layer-assembled nanoporous films as a highly stable platform for the fabrication of oligonucleotide SAM through one-step direct immobilization of the thiolated oligonucleotide probes on the Au NPs. MALDI-TOF MS analysis of covalently bound oligonucleotides has been achieved for the first time on a hybrid porous nanostructure comprising Au and SiO_2 NP assemblies. Important parameters include the SiO_2 NP-assembled nanoporous film and the existence of separate Au NPs. For comparison, a series of Au NP-assembled monolayers or nanoporous multilayers

have also been designed for the fabrication of DNA hybridization arrays. However, only the second and third hybridization strand complementary to the immobilized oligonucleotides could be measured by MALDI-TOF MS. Obtaining information about oligonucleotides' molecular weight within a DNA microarray is the first step toward detailed understanding of DNA or DNA fragments. These results have significant implications for the application of SAM technology in the detection of oligonucleotide hybridization on Au NP-based surfaces.

ACKNOWLEDGMENT

J.Z. acknowledges support from the National Natural Science Foundation of China (20604011, 20974044, 90923006), the National Basic Research Program of China (2007CB925103), and the Program for New Century Excellent Talents in University (NCET-06-0451).

SUPPORTING INFORMATION AVAILABLE

Additional information as noted in the text. This material is available free of charge via the Internet at http://pubs.acs.org.

Received for review June 23, 2009. Accepted September 16, 2009.

AC901815V